

FIELD DUE TO SOURCES IN THE IONOSPHERE  
AT VLF

by

Udo Karst

---

A Thesis Submitted to the Faculty of the  
DEPARTMENT OF ELECTRICAL ENGINEERING  
In Partial Fulfillment of the Requirements  
For the Degree of  
MASTER OF SCIENCE  
In the Graduate College  
THE UNIVERSITY OF ARIZONA

1 9 6 7

STATEMENT BY AUTHOR

This thesis has been submitted in partial fulfillment of requirements for an advanced degree at The University of Arizona and is deposited in the University Library to be made available to borrowers under rules of the Library.

Brief quotations from this thesis are allowable without special permission, provided that accurate acknowledgment of source is made. Requests for permission for extended quotation from or reproduction of this manuscript in whole or in part may be granted by the head of the major department or the Dean of the Graduate College when in his judgement the proposed use of the material is in the interests of scholarship. In all other instances, however, permission must be obtained from the author.

SIGNED: Udo Karst

APPROVAL BY THESIS DIRECTOR

This thesis has been approved on the date shown below:

George Tyras  
GEORGE TYRAS  
Associate Professor of Electrical Engineering

6/16/67  
Date

## ACKNOWLEDGMENTS

The author is greatly indebted to Dr. George Tyras for his helpful guidance and advice in the preparation of this thesis.

Thanks must also be extended to Dr. Harvey Cohn and the Mathematics Department for the use of their electronic computer.

This work was supported by the National Science Foundation through Research Grant GP-2307.

## TABLE OF CONTENTS

	Page
LIST OF ILLUSTRATIONS . . . . .	v
ABSTRACT . . . . .	vi
1. INTRODUCTION . . . . .	1
2. DISCUSSION OF THE PROBLEM . . . . .	3
2.1 Problem Statement . . . . .	3
2.2 The Source . . . . .	3
2.3 The Magnetoplasma . . . . .	4
2.4 The Boundaries . . . . .	6
3. PROBLEM FORMULATION . . . . .	8
3.1 The Field Equations . . . . .	8
3.2 The Boundary Conditions . . . . .	11
4. EVALUATION OF THE INTEGRAL . . . . .	14
4.1 The Integral Representation . . . . .	14
4.2 Expansion of the Reflection Coefficient . . . . .	17
4.3 Integral Evaluation on the Steepest Descent Path . . . . .	18
4.3a Introduction . . . . .	18
4.3b The Transformation $\lambda = \sqrt{x} \cos w$ . . . . .	21
4.3c The Transformation $\lambda = \sin \beta$ . . . . .	25
5. NUMERICAL RESULTS . . . . .	28
6. THE EAST-WEST EFFECT . . . . .	35
6.1 Introduction . . . . .	35
6.2 Physical Concepts . . . . .	36
6.3 Origin of the Nonreciprocity . . . . .	37
6.4 The Lossless Ionosphere . . . . .	42
6.5 Conclusion . . . . .	42
7. SUMMARY AND CONCLUSION . . . . .	44
REFERENCES . . . . .	46

# LIST OF ILLUSTRATIONS

Figure		Page
2.1	Geometry of the Problem . . . . .	13
4.1	Singular Points in the $\lambda$ -plane . . . . .	15
4.2	The Network of Image Sources . . . . .	19
4.3	Deformed Path of Integration in the $\lambda$ -plane . . .	20
4.4	Branch Cut Integration in the $w$ -plane . . . . .	22
4.5	Path of Integration in the $\beta$ -plane . . . . .	26
5.1	Calculated Field Strength at Close Range . . . . .	30
5.2	Experimental Results for 18.6 KHz . . . . .	31
5.3	Calculated Field Strength . . . . .	32
5.4	Experimental Results for 16.6 KHz . . . . .	33
5.5	The East-West Effect . . . . .	34
6.1	Plane Wave Incident Upon the Air-Ionosphere Boundary . . . . .	40

## ABSTRACT

The propagation of very low frequency (vlf) radiowaves in the earth-ionosphere waveguide region is considered. The earth is assumed flat and perfectly conducting while the ionosphere is sharply bounded, homogeneous, and anisotropic. The problem is formulated exclusively for propagation of the TM mode along the magnetic equator. The integral representation of the field is given and its characteristics are discussed with respect to the complex plane. A conformal transformation and the method of steepest descents are employed to evaluate the integral and obtain a final answer. The results are compared with experimental data in several field strength versus distance plots. The east-west effect is discussed at length and a detailed account of its origin in the air-ionosphere boundary is given.

## INTRODUCTION

The propagation of radio waves at vlf was understood fairly well as long ago as 1911. At that time the empirical Austin-Cohen formula was proposed. It described radio wave propagation quite accurately at about 25 KHz. Somewhat later vlf waves were studied experimentally by Round et al. (1925). Their findings indicated among other things that the propagation of radiowaves is, in general, nonreciprocal. This was labeled the east-west effect.

However, despite the fact that vlf waves propagate great distances with small attenuation, investigation into their nature was neglected for some time. More recently they have regained attention. The great need for satellite communication, long range navigation, and weather observation has again made very low frequencies desirable. Among others, Budden (1951, 1954) has studied the reflections of waves at the boundary of the ionosphere as also has Yabroff (1957). Wait (1957) and Wait and Howe (1957) have contributed significantly to the mode theory of wave propagation, while Crombie (1958), and Barber and Crombie (1959) have investigated the non-reciprocity of the reflection coefficient at the earth-ionosphere boundary. The same nonreciprocal property of the ionosphere boundary but in terms of its input admittance has been considered by Dobrott and Ishimaru (1961).

In this thesis the propagation of vlf waves in the air region between the earth and ionosphere due to a source located in the ionosphere will be discussed. The fields in the plasma medium are, in general, described by a set of coupled differential equations. In order to uncouple these equations the source excitation is chosen so that only one magnetic field component, parallel to the steady magnetic field is present. This is really no great restriction since it is just the transverse component of the earth's magnetic field that is important in vlf wave propagation to great distances.

In addition, the direction of propagation is taken along the magnetic equator. It is here where the greatest anisotropy occurs (Wait and Spies, 1960) and hence where the greatest difference in east-west propagation manifests itself. This east-west effect will be discussed in great detail. The method formulated by Barber and Crombie (1959) for the case of a plane wave incident upon the ionosphere will be employed to show not only that the electric vector in the plasma contains a rotating component, but also that this component is an absolute necessity for a nonreciprocity to occur.

It will also be seen that in the hypothetical case of a lossless ionosphere the east-west effect may or may not appear.



## 2. DISCUSSION OF THE PROBLEM

### 2.1 Problem Statement

The geometry of the problem is shown in Fig. 2.1. The plane  $z=0$  represents the earth's surface and the plane  $z=b$  a sharply bounded ionosphere. Region (0), then, is the earth-ionosphere waveguide. Region (1) is the ionosphere, semi-infinite in extent. For simplicity the curvatures of the earth and ionosphere are neglected and the earth's conductivity is considered infinite.

Excitation of electromagnetic waves is by a magnetic line source located in the ionosphere parallel to the interface and carrying a magnetic current  $I_m e^{-i\omega t}$  in the positive x-direction. A magnetostatic field  $H_{dc}$  parallel to the line source is present. Evaluation of field strength in the waveguide region is desired.

### 2.2 The Source

The source is an infinite magnetic line of current oriented in the x-direction, parallel to the earth's magnetic field. This type of excitation yields a magnetic field component in the x-direction and components of the electric field in the y-z plane. Hence the earth's magnetic field is parallel to the magnetic field of the wave and perpendicular to the direction of propagation. This case is of most importance in the transmission of vlf waves to great distances. The chosen excitation also results in uncoupled field equations which simplifies the problem though retaining the salient features.

A mathematical representation of the source is

$$\vec{j}_m = I_m \delta(y) \delta(z-b-h) \hat{x}$$

where  $\delta$  is the Dirac delta function and  $\hat{x}$  is a unit vector in the positive x-direction.

### 2.3 The Magnetoplasma

For the purpose of this thesis the ionosphere shall consist of an equal number of positive and negative charges, the positive ions and the electrons. Since the mass of the positive ions is appreciable compared to the electrons, the electrons only shall be considered free to move. The presence of a steady magnetic field renders the plasma anisotropic. Such a plasma may be characterized by the constitutive relations

$$\begin{aligned}\vec{D} &= \epsilon_0 \vec{\epsilon} \vec{E} \\ \vec{B} &= \mu_0 \mu \vec{H}\end{aligned}$$

where  $\vec{\epsilon}$  is the permittivity tensor given by (Tyras and Held, 1959):

$$\vec{\epsilon} = \begin{bmatrix} \epsilon & 0 & 0 \\ 0 & \epsilon & i\eta \\ 0 & -i\eta & \epsilon \end{bmatrix}$$

The different elements are complex. If one prime is used to denote the real part and two primes the imaginary, the different elements may be written:

$$\epsilon' = 1 - \frac{\omega_p^2}{\omega^2 + \nu^2}$$

$$\epsilon'' = \frac{\nu \omega_p^2}{\omega(\omega^2 + \nu^2)}$$

$$\epsilon' = 1 - \frac{\omega_p^2 (\omega^2 - \omega_H^2 + \nu^2)}{[(\omega + \omega_H)^2 + \nu^2][(\omega - \omega_H)^2 + \nu^2]}$$

$$\epsilon'' = \frac{\nu \omega_p^2 (\omega^2 + \omega_H^2 + \nu^2)}{\omega [(\omega + \omega_H)^2 + \nu^2][(\omega - \omega_H)^2 + \nu^2]}$$

$$\eta' = \frac{\omega_H \omega_p^2 (\omega^2 - \omega_H^2 - \nu^2)}{\omega [(\omega + \omega_H)^2 + \nu^2][(\omega - \omega_H)^2 + \nu^2]}$$

$$\eta'' = \frac{2\nu \omega_H \omega_p^2}{[(\omega + \omega_H)^2 + \nu^2][(\omega - \omega_H)^2 + \nu^2]}$$

where  $\omega_p$  is called the plasma frequency given by :

$$\omega_p^2 = \frac{e^2 N}{\epsilon_0 m_e}$$

and  $\omega_H$  is the cyclotron frequency given by :

$$\omega_H = - \frac{1.61 \mu_e H_{dc}}{m_e}$$

In these expressions  $N$  is the number of free electrons per cubic meter,  $|e| = 1.6 \times 10^{-19}$  coulomb is the electric charge,  $m_e = 9.1 \times 10^{-31}$  kg is the electron mass, and  $\omega$ ,  $\nu$  are the wave frequency and electron collision frequency, respectively.

The inverse of the permittivity tensor, which will be necessary in subsequent chapters, may be written:

$$\vec{\epsilon}^{-1} = \frac{1}{\chi} \begin{bmatrix} \frac{\chi}{\epsilon} & 0 & 0 \\ 0 & 1 & -iK \\ 0 & iK & 1 \end{bmatrix}$$

where  $\chi = \frac{\epsilon^2 - \eta^2}{\epsilon}$  and  $K = \frac{\eta}{\epsilon}$ .

## 2.4 The Boundaries

The lower boundary at  $z=0$  is the flat earth with the conductivity considered infinite. This is a good representation, for example, for a large expanse of ocean.

The boundary at  $z=b$  is the sharply bounded ionosphere. This, of course, is an idealization since the boundary is continuously varying. In fact, typical experimental results as reported by a colleague (Schell, 1967) yield the following variation in the parameter  $\chi$ , which for TM mode propagation is the square of the refractive index.

$$\chi = 0.9987 + 10.3215 \quad \text{at } z = 60 \text{ km}$$

$$\chi = 0.8822 + 16.176 \quad \text{at } z = 70 \text{ km}$$

$$\chi = -2.864 + 1136.1 \quad \text{at } z = 80 \text{ km}$$

These measurements were made at 11.14 KHz. The index of refraction,  $\sqrt{\chi}$ , then, changes from  $\sim 1.0$  to  $\sim 10$  in a half wavelength. Hence, considering the boundary to be abrupt at vlf is justified. It may be noted that the situation of vlf radiation incident on the

ionosphere is analogous to radiation of optical frequencies incident upon a metal plate. This aspect of the problem will be discussed further in Chapter 6.

### 3. PROBLEM FORMULATION

#### 3.1 The Field Equations

Since the main interest lies in finding the fields in the air space  $0 \leq z \leq b$  a solution to Maxwell's equations is implied. This solution must obey certain boundary conditions and exhibit a proper behavior at infinity. The formulation presented here has already been detailed by Tyras, Ishimaru, and Swarm (1963), and Wade and Williams (1966) and will only be sketched briefly.

Since the source current has a harmonic time dependence, Maxwell's equations yield the vector wave equation

$$(\vec{\nabla} \times \vec{\epsilon}^{-1} \vec{\nabla} \times - k_0^2) \vec{H}_1 = i\epsilon_0 \omega \vec{I}_m \delta(y) \delta(z-b-h) \hat{x}$$

The operation  $(\vec{\nabla} \times \vec{\epsilon}^{-1} \vec{\nabla} \times)$  may be written as a matrix if it is observed that:

$$\vec{\nabla} \times = \begin{bmatrix} 0 & -\partial_z & \partial_y \\ \partial_z & 0 & -\partial_x \\ -\partial_y & \partial_x & 0 \end{bmatrix} \quad (3.1)$$

Since the geometry of the problem precludes variation in the x coordinate

$$\partial_x = 0$$

Therefore a family of equations appears.

$$\begin{bmatrix} -[\partial_z^2 + \partial_y^2] \frac{1}{\epsilon} - k_0^2 & 0 & 0 \\ 0 & -\partial_z^2 (\frac{1}{\epsilon}) - k_0^2 & \partial_x \partial_y (\frac{1}{\epsilon}) \\ 0 & \partial_y \partial_z (\frac{1}{\epsilon}) & -\partial_y^2 (\frac{1}{\epsilon}) - k_0^2 \end{bmatrix} \begin{bmatrix} H_{x1} \\ H_{y1} \\ H_{z1} \end{bmatrix} = \begin{bmatrix} \hat{x} \\ 0 \\ 0 \end{bmatrix}$$

It is seen immediately that the y- and z-components are coupled but the x-component is uncoupled. Since, as has been concluded by previous research (Galejs and Row, 1964), the boundary conditions may be satisfied by an x-component only, the differential equation containing  $H_x$  will be sufficient and only  $H_x$  will appear in the final answer. This is a direct result of the nature and direction of source and steady magnetic field employed. Hence,

$$(\partial_z^2 + \partial_y^2 + \chi k_o^2) H_{x1} = -i\epsilon_o \omega \chi I_m \delta(y) \delta(z-b-h) \quad (3.2)$$

Likewise for the air space

$$(\partial_z^2 + \partial_y^2 + k_o^2) H_{x0} = 0 \quad (3.3)$$

In order to solve the above equations, the Fourier transform pair is introduced.

$$\tilde{F}(z, \alpha) = \int_{-\infty}^{\infty} F(z, y) e^{-i\alpha y} dy \quad (3.4)$$

$$F(z, y) = \int_{-\infty}^{\infty} \tilde{F}(z, \alpha) e^{i\alpha y} \frac{d\alpha}{2\pi} \quad (3.5)$$

Applying (3.4) to (3.2) and (3.3) in the usual manner yields:

$$-(d_z^2 + [\chi k_o^2 - \alpha^2]) \tilde{H}_{x1} = i\epsilon_o \omega \chi I_m \delta(z-b-h) \quad (3.6)$$

$$(d_z^2 + [k_o^2 - \alpha^2]) \tilde{H}_{x0} = 0 \quad (3.7)$$

The most general solution of (3.7) is the complimentary solution

$$\tilde{H}_{x_0} = A_0 e^{i s_0 z} + B_0 e^{-i s_0 z} \quad (3.8)$$

Since (3.6) has a source term there will be a complimentary solution

$$\tilde{H}_c = A_1 e^{i s_1 z} + B_1 e^{-i s_1 z} \quad (3.9)$$

and a particular solution

$$\tilde{H}_\rho = -\frac{1}{2} \epsilon_0 \omega \chi \operatorname{Im} \frac{e^{i s_1 |z - (b+h)|}}{s_1} \quad (3.10)$$

where the coefficients are functions of the transform variable,  $\alpha$ ,

and

$$s_0 \equiv \sqrt{k_0^2 - \alpha^2}$$

$$s_1 \equiv \sqrt{\chi k_0^2 - \alpha^2}$$

It is necessary at this point to establish a sign convention concerning the radicals. It shall be required that

$$\operatorname{Im}\{s_0\} \geq 0; \operatorname{Im}\{s_1\} \geq 0 \quad (3.11)$$

This in effect chooses the upper surface of the Riemann plane.

With this information it is seen immediately that  $B_1$  in (3.9) must be zero. This follows since  $z$  is unbounded in the positive direction in medium (1). A  $B_1 \neq 0$  would result in  $H_{1c} \rightarrow \infty$  as  $z \rightarrow \infty$  which is physically impossible. Therefore the transformed fields become:



$$\tilde{H}_{x0} = A_0 e^{i s_0 z} + B_0 e^{-i s_0 z} \quad (3.8)$$

$$\tilde{H}_{x1} = -\frac{1}{2} \epsilon_0 \omega \chi I_m \frac{e^{i s_1 |z-(b+h)|}}{s_1} + A_1 e^{i s_1 z} \quad (3.12)$$

Now applying the inverse Fourier transform (3.5) the fields become

$$H_{x0} = -\frac{\omega \epsilon_0 \chi I_m}{4\pi} \int_{-\infty}^{\infty} [A_0 e^{i s_0 z} + B_0 e^{-i s_0 z}] e^{i \alpha y} d\alpha \quad (3.13)$$

$$H_{x1} = -\frac{\omega \epsilon_0 \chi I_m}{4\pi} \int_{-\infty}^{\infty} \left[ \frac{e^{i s_1 |z-(b+h)|}}{s_1} + A_1 e^{i s_1 z} \right] e^{i \alpha y} d\alpha \quad (3.14)$$

where the coefficients  $A_0$ ,  $B_0$ , and  $A_1$  have been renormalized for convenience.

Equations (3.13) and (3.14) are in effect the answers. First, however, the coefficients must be evaluated by applying the boundary conditions which will now be discussed briefly.

### 3.2 The Boundary Conditions

The boundary conditions are:

$$E_{T0} = 0 \quad \text{at } z = 0 \quad (3.15)$$

since  $z = 0$  is a perfect conductor and

$$\left. \begin{aligned} E_{T1} &= E_{T0} \\ H_{T1} &= H_{T0} \end{aligned} \right\} \text{at } z = b \quad (3.16)$$

$$H_{T1} = H_{T0} \quad (3.17)$$

where the subscript T in each case denotes the components tangential to the boundary. It will be convenient to express these conditions completely in terms of the magnetic field. Using Maxwell's equations in source-free region (0) the boundary condition (3.15) becomes

$$\partial_z H_{x0} = 0 \quad \text{at } z = 0 \quad (3.18)$$

Similarly in source-free region (1)

$$\vec{\nabla} \times \vec{H} - \epsilon_0 \vec{E} \frac{\partial \vec{E}}{\partial t} = 0 \quad (3.19)$$

Expressing (3.19) in matrix form yields:

$$\begin{bmatrix} E_{x1} \\ E_{y1} \\ E_{z1} \end{bmatrix} = \frac{i}{\epsilon_0 \omega \chi} \begin{bmatrix} \frac{\chi}{\xi} & 0 & 0 \\ 0 & 1 & -iK \\ 0 & iK & 1 \end{bmatrix} \begin{bmatrix} 0 \\ \partial_z H_{x1} \\ -\partial_y H_{x1} \end{bmatrix} \quad (3.20)$$

Observing that

$$\partial_y H_{x1} = i\alpha H_{x1} \quad (3.21)$$

allows (3.16) to be written as:

$$\chi \partial_z H_{x0} = (\partial_z - K\alpha) H_{x1} \quad \text{at } z = b \quad (3.22)$$

It is now a simple matter to solve for  $A_0$ ,  $B_0$ , and  $A_1$  by applying boundary conditions (3.17), (3.18), and (3.22).

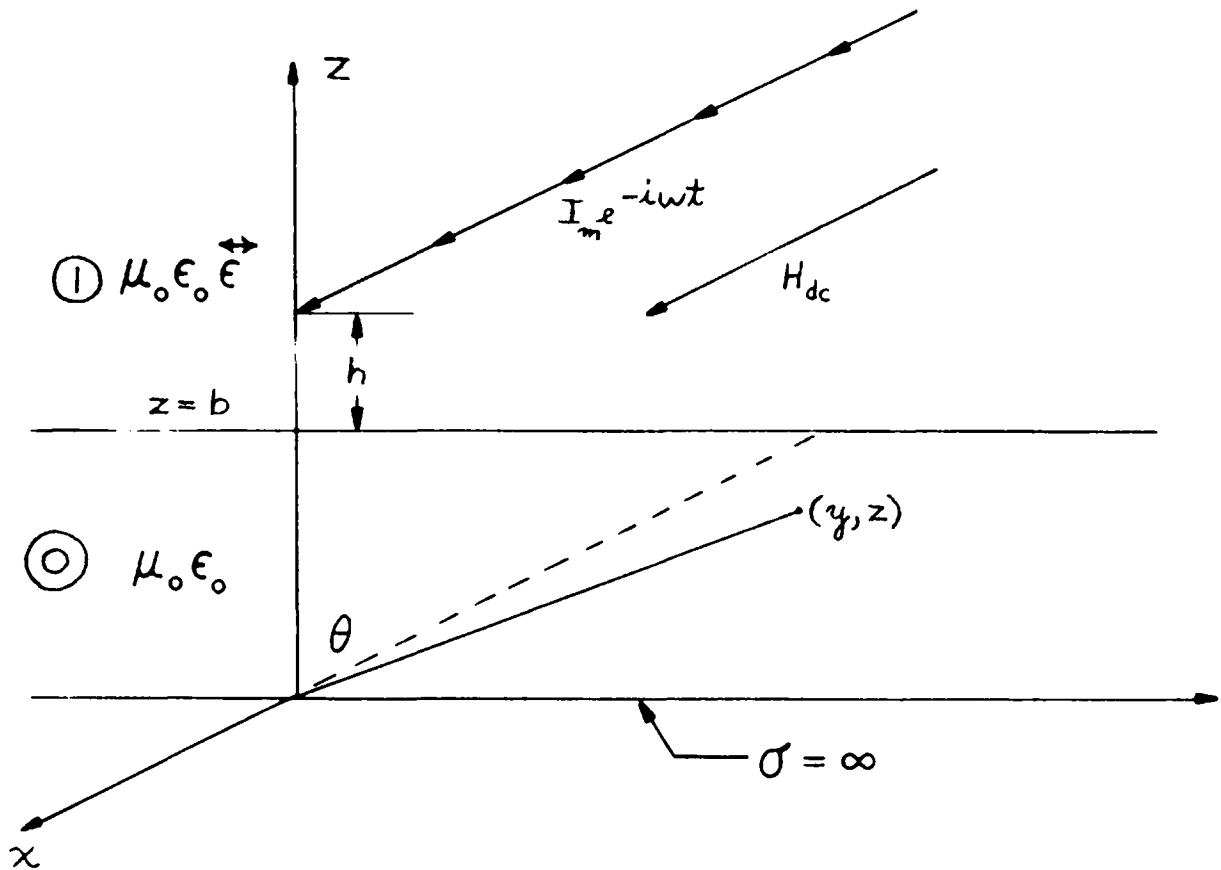


Figure 2.1 Geometry of the Problem

#### 4. EVALUATION OF THE INTEGRAL

##### 4.1 The Integral Representation

The integral (3.13) in the waveguide region is of importance and may be written:

$$H_{x0} = \frac{-\epsilon_0 \omega \chi I_m}{2\pi} \int_{-\infty}^{\infty} \frac{e^{is_1 h} e^{is_0 b} (e^{is_0 z} + e^{-is_0 z}) e^{i\alpha y} d\alpha}{[\chi s_0 + (s_1 + i\kappa\alpha)][1 - R e^{i2s_0 b}]}$$

where  $R$  is the reflection coefficient at the air-plasma interface given by

$$R = \frac{\chi s_0 - (s_1 + i\kappa\alpha)}{\chi s_0 + (s_1 + i\kappa\alpha)}$$

The reflection coefficient at the earth boundary is, of course, unity. If, now, the transformation

$$\alpha = k_0 \lambda$$

is applied to the integral above, the result is:

$$H_{x0} = \frac{-\epsilon_0 \omega \chi I_m}{2\pi} \int_{-\infty}^{\infty} \frac{e^{ik_0 h \sqrt{1-\lambda^2}} e^{ik_0 b \sqrt{1-\lambda^2}} (e^{iz\sqrt{1-\lambda^2}} + e^{-iz\sqrt{1-\lambda^2}}) e^{ik_0 \lambda y} d\lambda}{[\chi \sqrt{1-\lambda^2} + (\sqrt{1-\lambda^2} + i\kappa\lambda)][1 - R(\lambda) e^{i2k_0 b \sqrt{1-\lambda^2}}]} \quad (4.1)$$

It will be profitable to inspect this representation in the complex plane. If the singularities in the integrand are plotted in the  $\lambda$ -plane Fig. 4.1 results. It is seen that  $\lambda = \pm \sqrt{x}$  yields two branch points which are connected by a branch cut passing through infinity. The poles are located by the expression  $1 - R(\lambda) e^{i2k_0 b \sqrt{1-\lambda^2}} = 0$ .

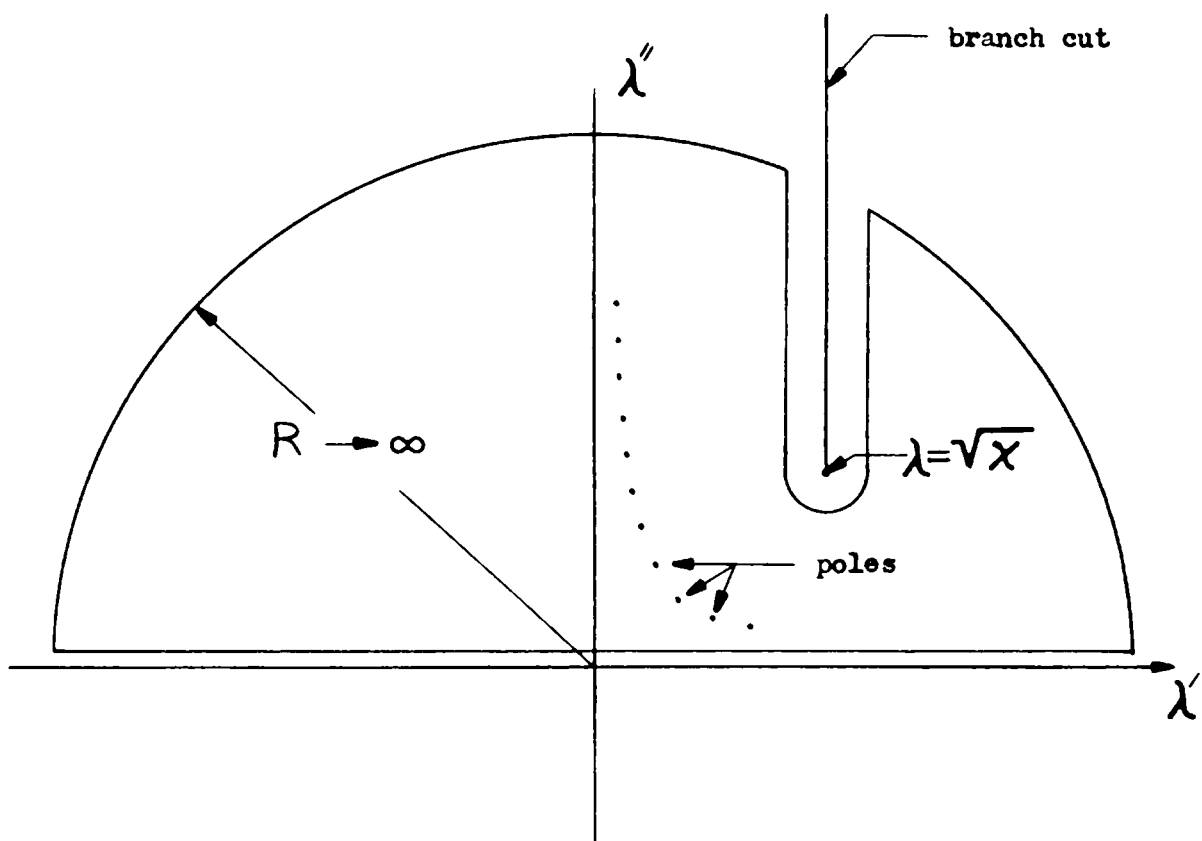


Figure 4.1 Singular Points in the  $\lambda$ -plane

The path of integration runs along the  $\lambda'$ -axis from  $-\infty$  to  $+\infty$  and closes in the top half-plane with a semicircle. It is obvious at once that the contour must be indented around the branch cut emanating from  $\lambda = +\sqrt{x}$  and proceeding upward to infinity. The contour of integration may be deformed in all portions of the complex plane where the function is analytic. Therefore, the integral (4.1) may be written as the sum of the contributions from the poles and the branch cut.

$$H_x = H_m + H_{bc}$$

Here  $H_m$  is called the modal field and  $H_{bc}$  contributes a so called lateral wave (Brekhovskikh, 1960).

This type of approach is called the mode theory of wave propagation since the contribution from each pole corresponds to a particular mode. In general, a few poles will lie between the  $\lambda''$ -axis and the  $\lambda = 1$  point, close to the  $\lambda'$ -axis. These poles will contribute the major portion to the field and may be called the dominant modes. The remaining poles, infinite in number, contribute only negligibly to the total field.

The integration around the branch cut yields, as noted, a lateral wave. It may in certain instances be the dominant term but in general, and as will be shown subsequently, the lateral wave falls off exponentially and will therefore not contribute significantly.

In addition to the mode theory outlined above another interpretation of the integral is available. This second interpretation describes the field in the waveguide as a summation of contributions

from an infinite number of image sources. It will now be discussed and subsequently used to evaluate the integral.

#### 4.2 Expansion of the Reflection Coefficient

It is possible to assume on the path of integration that

$$|R e^{i 2 k_0 b \sqrt{1-\lambda^2}}| < 1$$

This is justified by the physical consideration that there will be some absorption, regardless of how small, of the incident wave in the boundary. (A notable exception is the case of tangential incidence,  $\theta \rightarrow \frac{\pi}{2}$ , in which case  $|R|=1$ ). Alternately a small imaginary part may be assigned to  $k_0$ . Upon these assumptions the term

$$(1 - R e^{i 2 k_0 b \sqrt{1-\lambda^2}})^{-1}$$

may be expanded in a power series according to:

$$(1-x)^{-1} = 1+x+x^2+x^3+\dots = \sum_{n=0}^{\infty} x^n \quad |x| < 1.$$

Using this expansion, (4.1) may be arranged as the sum of two terms (Brekhovskikh, 1960)

$$H_{x_0} = - \frac{\omega \epsilon_0 \lambda I_m}{2\pi} \sum_{n=0}^{\infty} \sum_{j=1}^2 I_{jn} \quad (4.2)$$

where

$$I_{1n} = \int_{-\infty}^{\infty} \frac{e^{i k_0 h \sqrt{x-\lambda^2}} e^{i k_0 [(1+2n)b+z]\sqrt{1-\lambda^2} + y\lambda}}{\lambda \sqrt{1-\lambda^2} + (\sqrt{x-\lambda^2} + i\kappa\lambda)} [R(\lambda)]^n d\lambda$$

and

$$I_{2n} = \int_{-\infty}^{\infty} \frac{e^{i k_0 h \sqrt{x-\lambda^2}} e^{i k_0 [(1+2n)b-z]\sqrt{1-\lambda^2} + y\lambda}}{\lambda \sqrt{1-\lambda^2} + (\sqrt{x-\lambda^2} + i\kappa\lambda)} [R(\lambda)]^n d\lambda$$

By considering the exponential portion containing  $\sqrt{1-\lambda^2}$  it is seen that the parameter  $z$  has been replaced by an "effective" value of  $z$  given by:

$$z_{jn} = (1+2n)b \pm z \quad j = 1, 2 \quad (4.3)$$

The plus sign corresponds to  $j = 1$  and the minus sign to  $j = 2$ . This interpretation yields the image source representation as shown in Fig. 4.2. In this case the reflection coefficient to the  $n$ -th power may be considered as a weighting function for the  $n$ -th source.

In either of the above representations it is seen that the field consists of an infinite number of integrals. These integrals are very similar and may be evaluated by an approximate method known as the method of steepest descents or saddle point method. This method is widely documented (Baños, 1966; Brekhovskikh, 1960; Tyras, 1963) and will not be discussed here.

#### 4.3 Integral Evaluation on the Steepest Descent Path

##### 4.3a Introduction

In Fig. 4.3 the  $\lambda$ -plane is again pictured, this time including not only the branch cut but also the assumed saddle point, the angle  $\theta$ , and the deformed path of integration, composed of two segments,  $\Gamma_1$  and  $\Gamma_2$ . It is seen immediately that for  $\theta \leq \theta_c$  the branch cut will not be crossed by the path of integration and the contribution due to the lateral wave will be zero. In this case evaluation of the integral along path  $\Gamma_1$  will result in the total field. At angles greater than  $\theta_c$  the contour  $\Gamma_1$  intercepts the branch



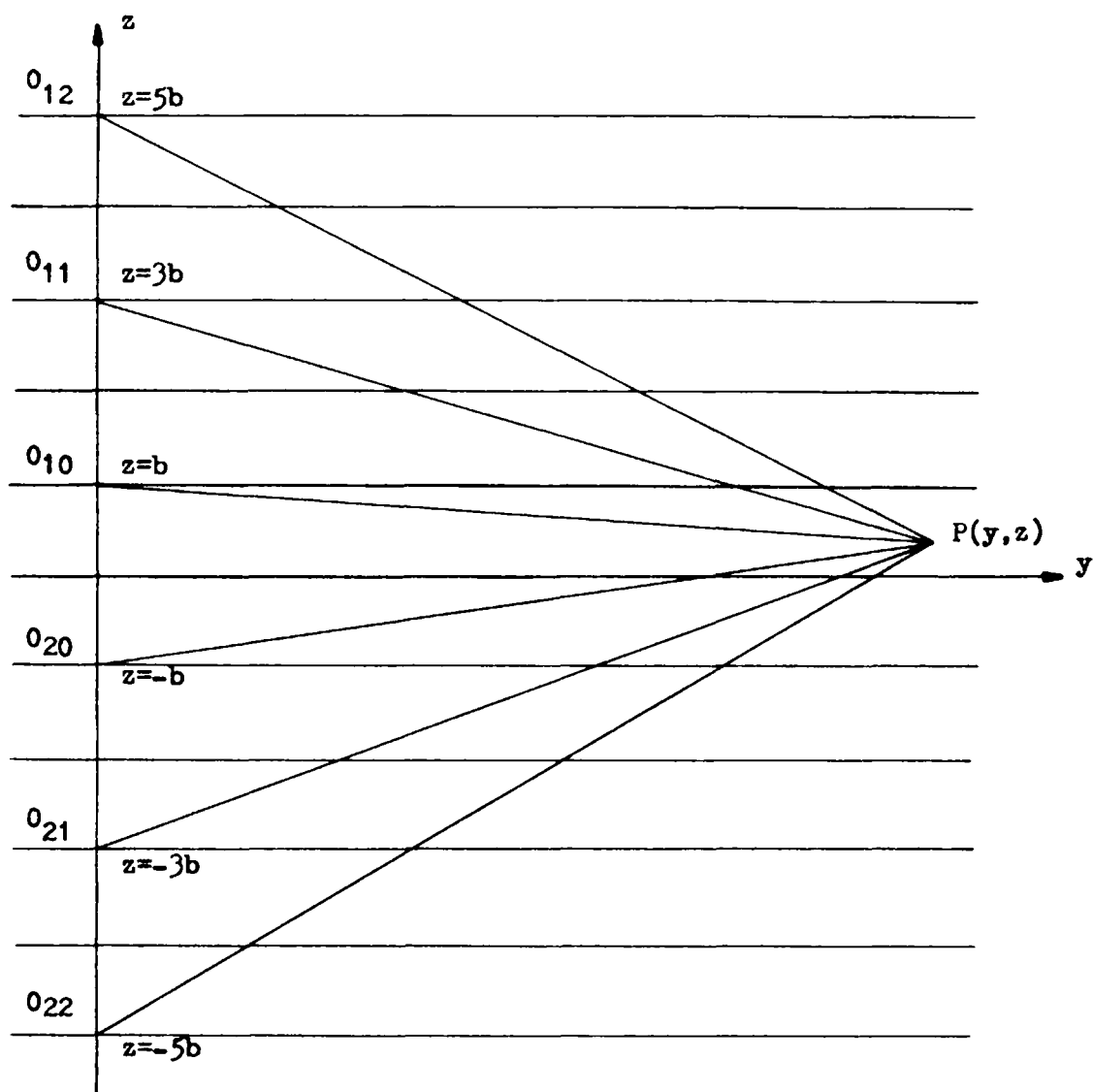


Figure 4.2 The Network of Image Sources

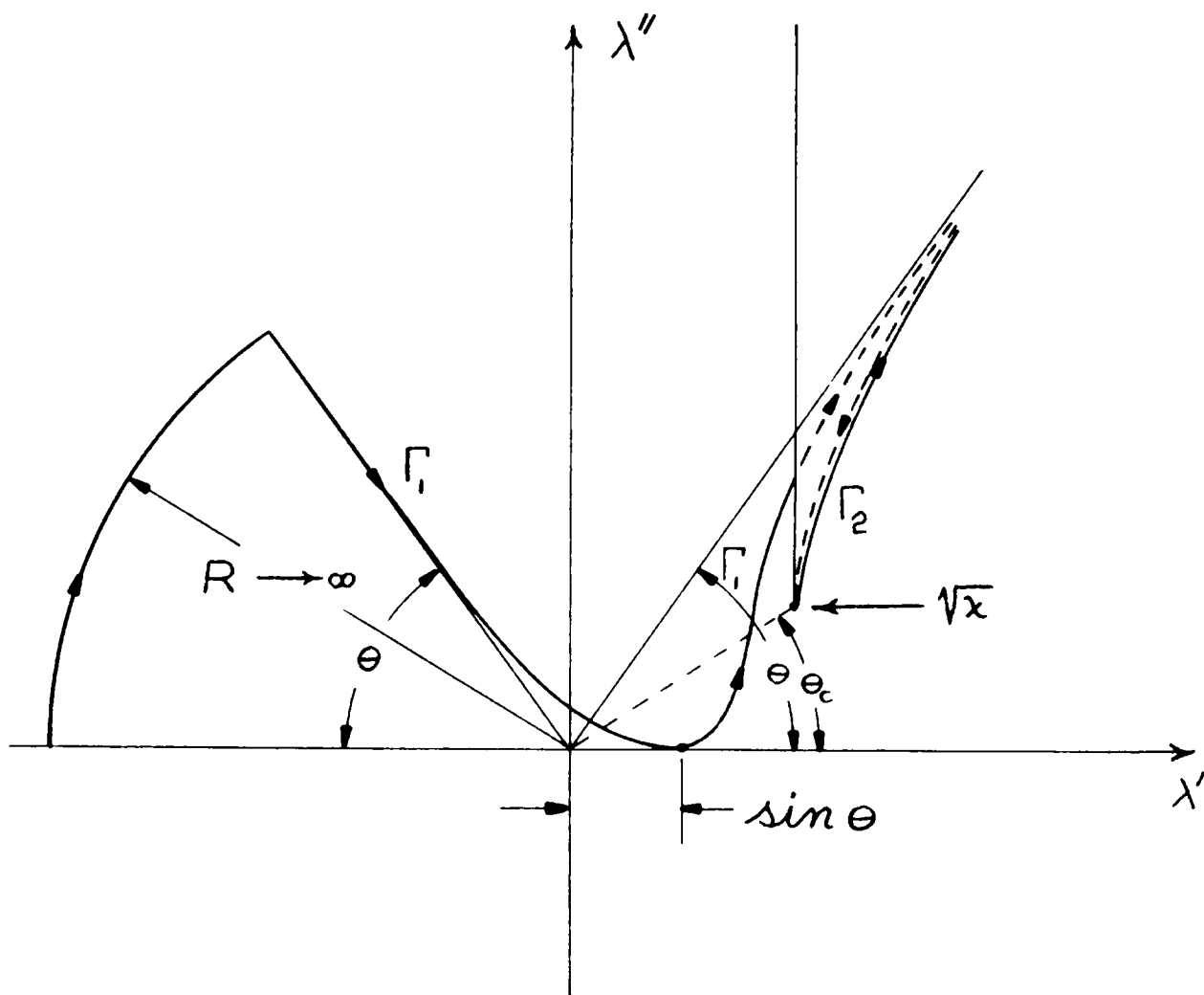


Figure 4.3 Deformed Path of Integration in the  $\lambda$ -plane

cut, however, and thus leaves the original Riemann sheet. In order to return to the same Riemann sheet the path  $\Gamma_2$  is necessary. The integration around this path is the lateral wave. It is therefore possible to write the total field as:

$$H_{x0} = H_{x0}^{\Gamma_1} + u(\theta - \theta_c) H_{x0}^{\Gamma_2} \quad (4.4)$$

where  $u(\theta - \theta_c)$  is the unit step function and  $\Gamma_1$ ,  $\Gamma_2$  denote the respective paths. An approximate value for  $\theta_c$  is readily available. In section 2.4 it was seen that  $\lambda$  had a very large imaginary part compared to the real part. It is therefore not a bad assumption to consider  $\lambda$  as pure imaginary. This would yield equal real and imaginary components for  $\sqrt{\lambda}$ . Hence

$$\theta_c \approx \frac{\pi}{4}$$

It shall now be shown that the integral over  $\Gamma_2$ , the lateral wave, decreases exponentially and hence is negligible.

#### 4.3b The Transformation $\lambda = \sqrt{\lambda} \cos w$

The transformation

$$\lambda = \sqrt{\lambda} \cos w \quad ; \quad d\lambda = -\sqrt{\lambda} \sin w dw \quad (4.5)$$

is made in the integral (4.2). As is seen in Fig. 4.4, the conformal transformation (4.5) maps the complete upper Riemann sheet of the  $\lambda$ -plane onto a strip of width  $\pi$  in the  $w$ -plane. The boundaries are the contours about the upper and lower branch cuts in the  $\lambda$ -plane.

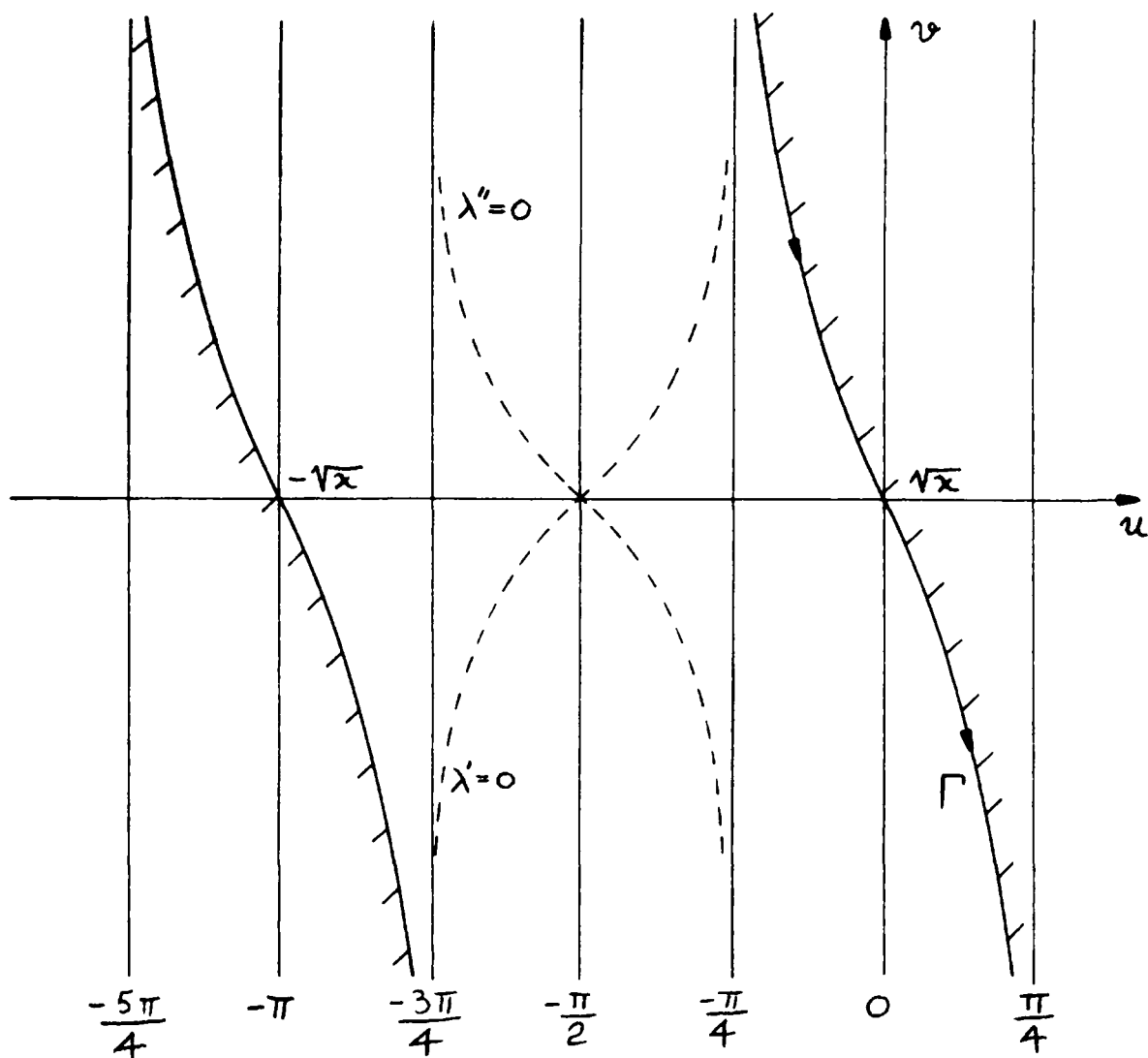


Figure 4.4 Branch Cut Integration in the  $w$ -plane

The equations of the boundaries can be deduced from the conditions  
(Baños, 1966)

$$\operatorname{Re}\{\sqrt{x} \cos w\} = \pm \operatorname{Re}\{\sqrt{x}\}$$

$$\operatorname{Im}\{\sqrt{x} \cos w\} \geq \pm \operatorname{Im}\{\sqrt{x}\}$$

and these are shown in their general curvilinear shape. The real and imaginary axes of the  $\lambda$ -plane have also been shown for reference. The desired path of integration is, of course, the right hand boundary  $\Gamma$ .

If in addition the space coordinates are transformed according to the suggestions of section 4.2 and equation (4.3)

$$\begin{aligned} y &= r_{jn} \sin \theta_{jn} \\ z_{jn} &= r_{jn} \cos \theta_{jn} \end{aligned} \quad (4.6)$$

the integral (4.2) becomes:

$$\begin{aligned} H_{x_0}^{\Gamma_2} &= - \frac{\omega \epsilon_0 x I_m}{2\pi} \sum_0^\infty \sum_1^2 F(w) e^{i k_0 r_{jn} [\cos \theta_{jn} \sqrt{1-x \cos^2 w}]} \\ &\quad \cdot e^{i k_0 r_{jn} [\sin \theta_{jn} \sqrt{x} \cos w]} dw \end{aligned} \quad (4.7)$$

where

$$F(w) = \frac{e^{i k_0 h \sqrt{x} \sin w} (-\sqrt{x} \sin w) [R(w)]^n}{x \sqrt{1-x \cos^2 w} + (\sqrt{x} \sin w + i k \sqrt{x} \cos w)} \quad (4.8)$$

Taking according to the method of steepest descents

$$f(w) = ik_0 (\cos \theta_{jn} \sqrt{1 - \lambda \cos^2 w} + \sin \theta_{jn} \sqrt{\lambda} \cos w)$$

two roots occur at

$$w = 0, \quad w = \arccos\left(\frac{1}{\sqrt{\lambda}} \sin \theta_{jn}\right)$$

As is seen in Fig. 4.4, the proper saddle point is the first root.

The second one will refer to the integration over  $H_{x0}^{\Gamma}$ . Consequently employing the transformation

$$s^2 = ik_0 [\sin \theta_{jn} \sqrt{\lambda} + \cos \theta_{jn} \sqrt{1 - \lambda} - \sin \theta_{jn} \sqrt{\lambda} \cos w - \cos \theta_{jn} \sqrt{1 - \lambda} \cos^2 w]$$

yields for the field in (4.7):

$$H_{x0}^{\Gamma_2} = \frac{-\omega \epsilon_0 \lambda I_m}{2\pi} \sum_{n=0}^{\infty} \sum_{l=1}^2 e^{ik_0 r_{jn} \sqrt{\lambda} (\sin \theta_{jn} + i \cos \theta_{jn} \sqrt{1 - \lambda})}$$

$$\cdot \int_{-\infty}^{\infty} e^{r_{jn} s^2} \left\{ F[w(s)] \frac{dw}{ds} \right\} ds$$

The quantity in the braces may be expanded in powers of  $s$  and the subsequent integration yields a quickly converging series in inverse powers of  $r$ . The integrand, then, is bounded. Of primary importance now emerges the exponent. Since  $\sqrt{\lambda}$  has an appreciable imaginary part, the exponent will have a large negative real portion. Hence, especially if  $r$  is large, the field due to the branch cut integration,  $H_{x0}^{\Gamma_3}$ , will die out exponentially. This is equivalent to saying the lateral wave will not contribute to the total field.

The only contribution to the field will come from the first term in (4.4). This term will now be evaluated.

#### 4.3c The Transformation $\lambda = \sin \beta$

In order to evaluate the integral (4.2) on the contour  $\Gamma_1$ , the transformation

$$\lambda = \sin \beta, \quad d\lambda = \cos \beta d\beta$$

is made. The effect of this mapping is similar to the one just discussed in the previous section. Fig. 4.5 shows that the  $\lambda$ -plane has been mapped onto the infinite strip between  $-\frac{\pi}{2}$  and  $\frac{\pi}{2}$ . The path of integration, the  $\lambda'$ -axis, is shown as  $\Gamma_1$ . The branch point and branch cut are located well away from the path of integration. This results since  $\beta'' \gg 1$ . Actually in view of the results of the preceding section, the branch point may be ignored. Since there are no other singularities in the  $\beta$ -plane, the deformation to the path of steepest descents should occur without difficulty. And in fact it does.

Employing the transformation (4.6)

$$y = r_{jn} \sin \phi_{jn}$$

$$z_{jn} = r_{jn} \cos \phi_{jn}$$

yields for the field in (4.2):

$$H_{x0}^{\Gamma_1} = \frac{-\omega \epsilon_0 \chi I_m}{2\pi} \sum_{j=0}^{\infty} \sum_{n=1}^2 \int_{-\infty}^{\infty} F(\beta) e^{i k_0 r_{jn} \cos(\beta - \phi_{jn})} d\beta$$

$$F(\beta) = \frac{e^{i k_0 h \sqrt{\chi - \sin^2 \beta}} \cos \beta [R(\beta)]^n d\beta}{\chi \cos \beta + (\sqrt{\chi - \sin^2 \beta} + i \kappa \sin \beta)}$$

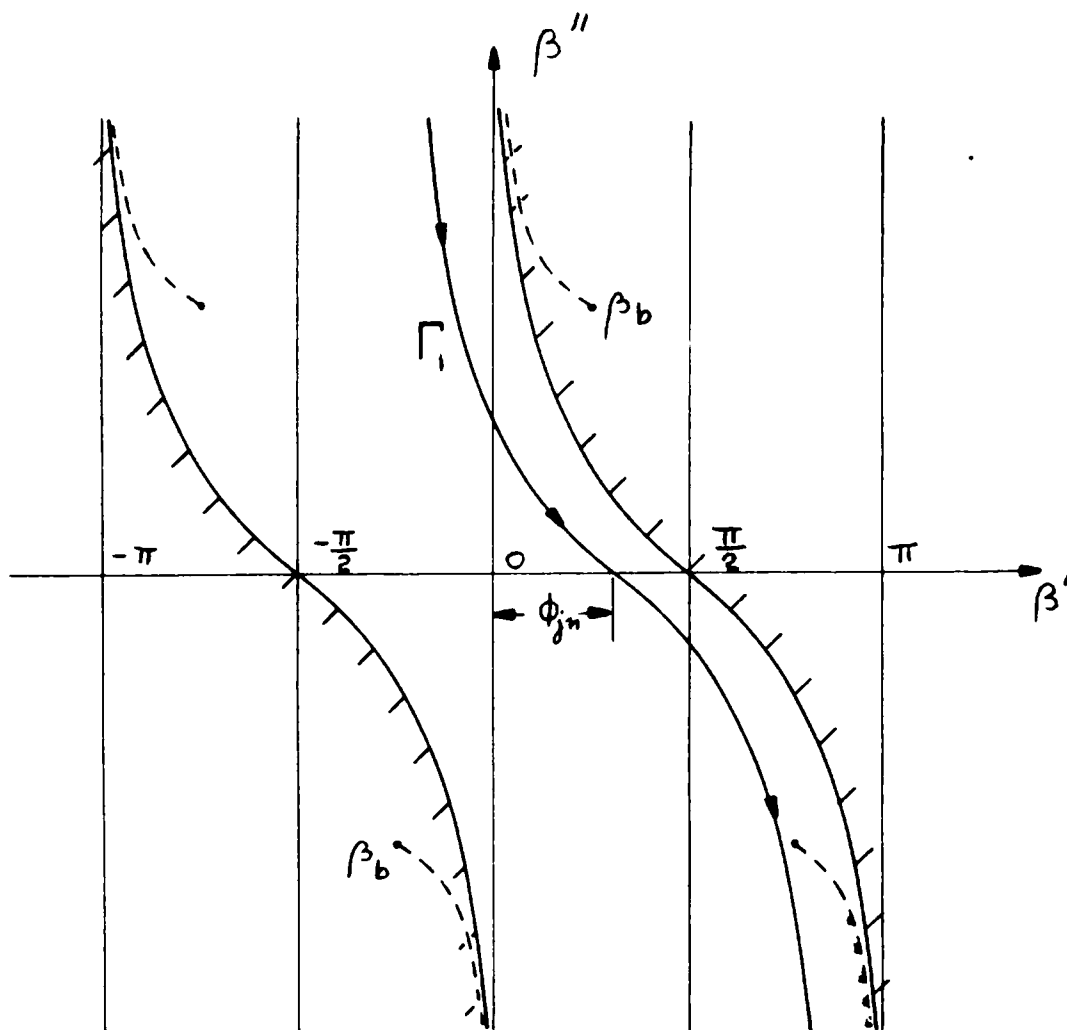


Figure 4.5 Path of Integration in the  $\beta$ -plane



From the exponent it is seen that

$$\beta = \phi_{jn} \quad (4.9)$$

is the desired saddle point. The path corresponding to this saddle point is shown in Fig. 4.5 as  $\Gamma_1$ . This is the path of steepest descents given by:

$$\cos(\beta - \phi_{jn}) = 1 + \frac{i}{k_0} s^2$$

Using the information (4.9) and employing the saddle point method, the field in the earth-ionosphere waveguide may be found.

$$H_{x_0} = \frac{-\omega \epsilon_0 \chi I_m}{2\pi} \sum_{j=0}^{\infty} \sum_1^2 e^{i k_0 (r_{jn} - \frac{\pi}{4})} \sqrt{\frac{2\pi}{k_0 r_{jn}}} \cdot \left[ \frac{e^{i k_0 h \sqrt{\chi - \sin^2 \phi_{jn}}} \cos \phi_{jn} [R(\phi_{jn})]^n}{\chi \cos \phi_{jn} + (\sqrt{\chi - \sin^2 \phi_{jn}} + i \kappa \sin \phi_{jn})} \right] \quad (4.10)$$

This answer is presented in graphical form in Figs. 5.1-5.5 and will be discussed in the next chapter.

## 5. NUMERICAL RESULTS

The final expression for the fields, (4.10), has been programmed for a digital computer and the results are plotted in the following figures. The ordinate in each case represents the field strength, measured on the ground, of a unit source located in the ionosphere. The abscissa is the distance from the source in kilometers. Also, in each theoretical graph the solid line represents the positive values of  $y$ , and the dashed lines negative values of  $y$ . The difference in the curves for the two directions is due to the east-west effect. This will be explained in great detail in the next chapter.

In order to check the results obtained a comparison with known experimental data is appropriate. Considerable amounts of information are not available, especially for propagation exactly along the magnetic equator. For the present purpose the data gathered by Heritage, Weisbrod, and Bickel, as presented at a Symposium of v.l.f. Radio Waves at Boulder, Colorado, Jan. 1957, and reported by Wait (1957, 1962) will be used.

Fig. 5.1 shows the field strength for the source located 10 m above the interface at a frequency of 11.14 KHz. At the distances shown the higher order modes still contribute significantly and are the cause of the marked interference effects observed. Fig. 5.2 is an experimental curve for comparison with Fig. 5.1. The field strength

recorded is that of the vlf transmitter (18.6 KHz) at Jim Creek, Washington taken in the direction of San Diego, California. The qualitative agreement is good. Especially the deep troughs at 250 km and 600 km, as well as the two peaks at about 750 km are observed in both plots

Fig. 5.3 again is a theoretical plot, this time for distances up to 5000 km. The experimental plot, Fig. 5.4 compares well. Fig. 5.4 is field strength taken in Dec. 1954 between San Diego, California and Hawaii at a frequency of 16.6 KHz. Again the major interference effects between 250 km and 900 km are clearly visible in both plots, indicating the general validity of the theoretical treatment. The attenuation of vlf radio waves, as found experimentally by Round et al. (1925), is about 3-4 db/K at 12.8 KHz. The attenuation determined from the theoretical plots (especially Fig. 5.5) was between 2.78 db/K and 3.67 db/K depending upon the direction of the path.

Fig. 5.5 also shows the marked difference between east-west and west-east propagation. It is seen that for west to east the attenuation is about 1 db/K less than in the opposite direction. The same phenomenon was observed by Round et al., who determined a difference of about 2 db/K. Since, however, their observations were sometimes over mixed land-sea paths, and also over day-night paths, and never due east-west, it is difficult to make a good comparison on this point.

As is seen from the preceding comparisons, the theoretical treatment employed appears entirely justified by the general agreement with experimental observations.

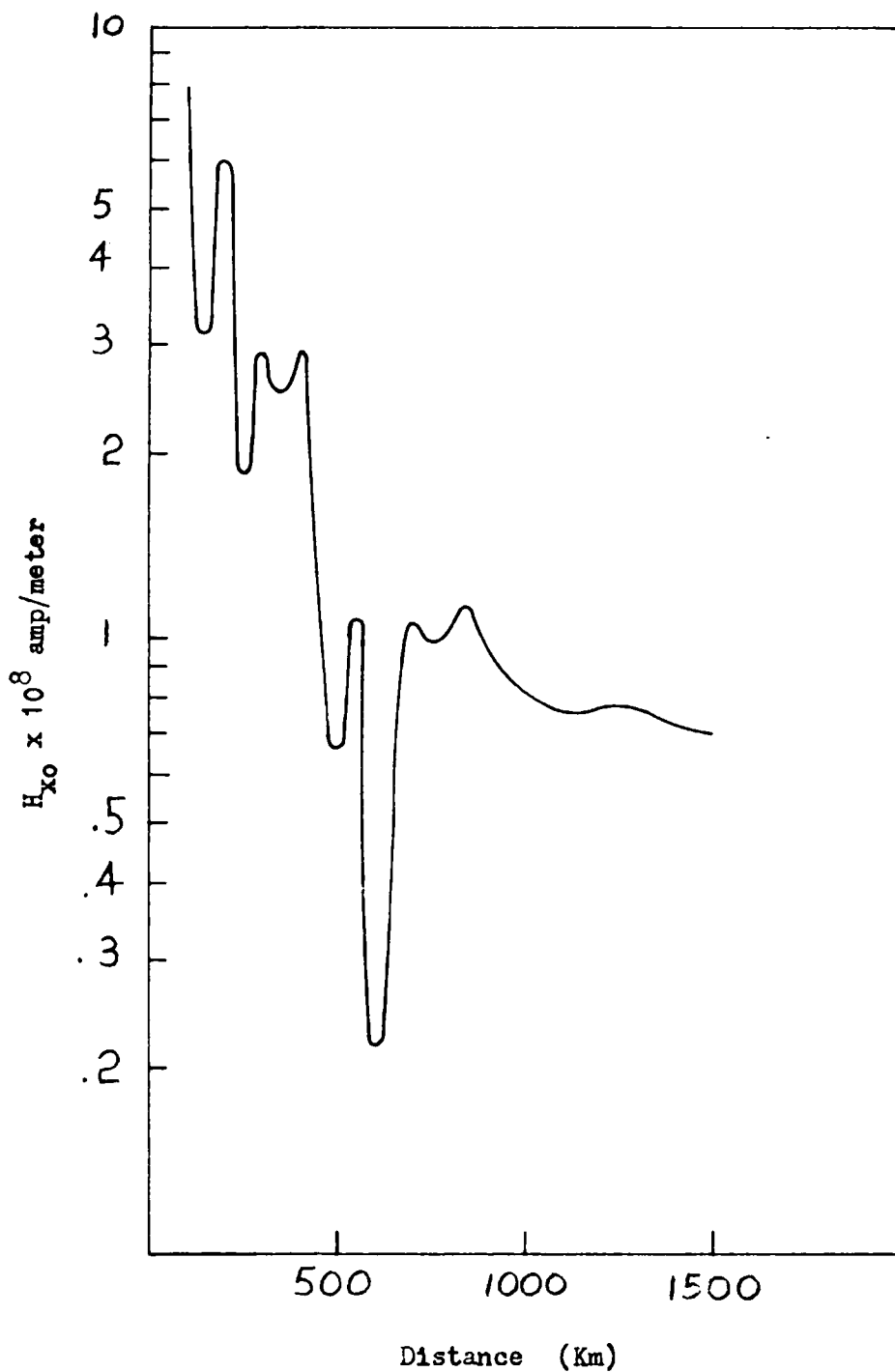


Figure 5.1 Calculated Field Strength at Close Range

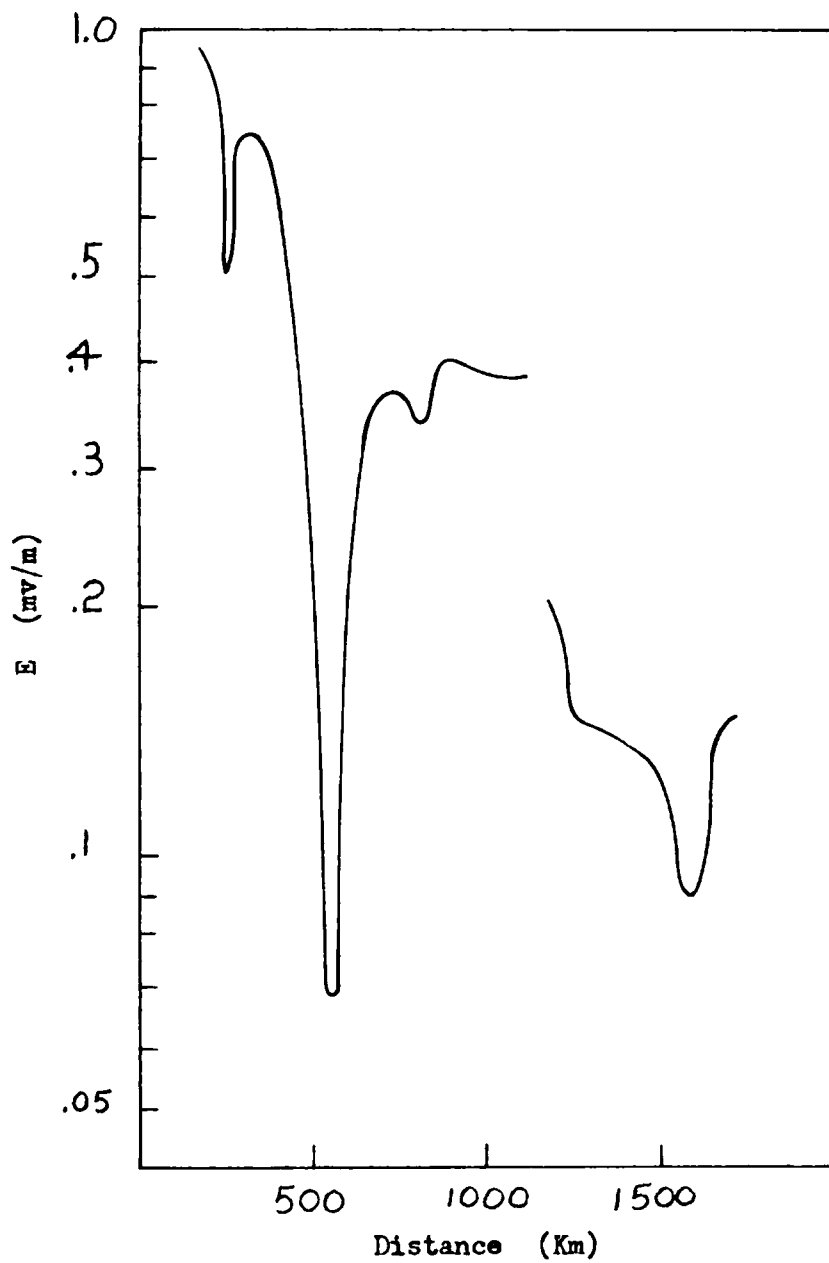


Figure 5.2 Experimental Results for 18.6 KHz

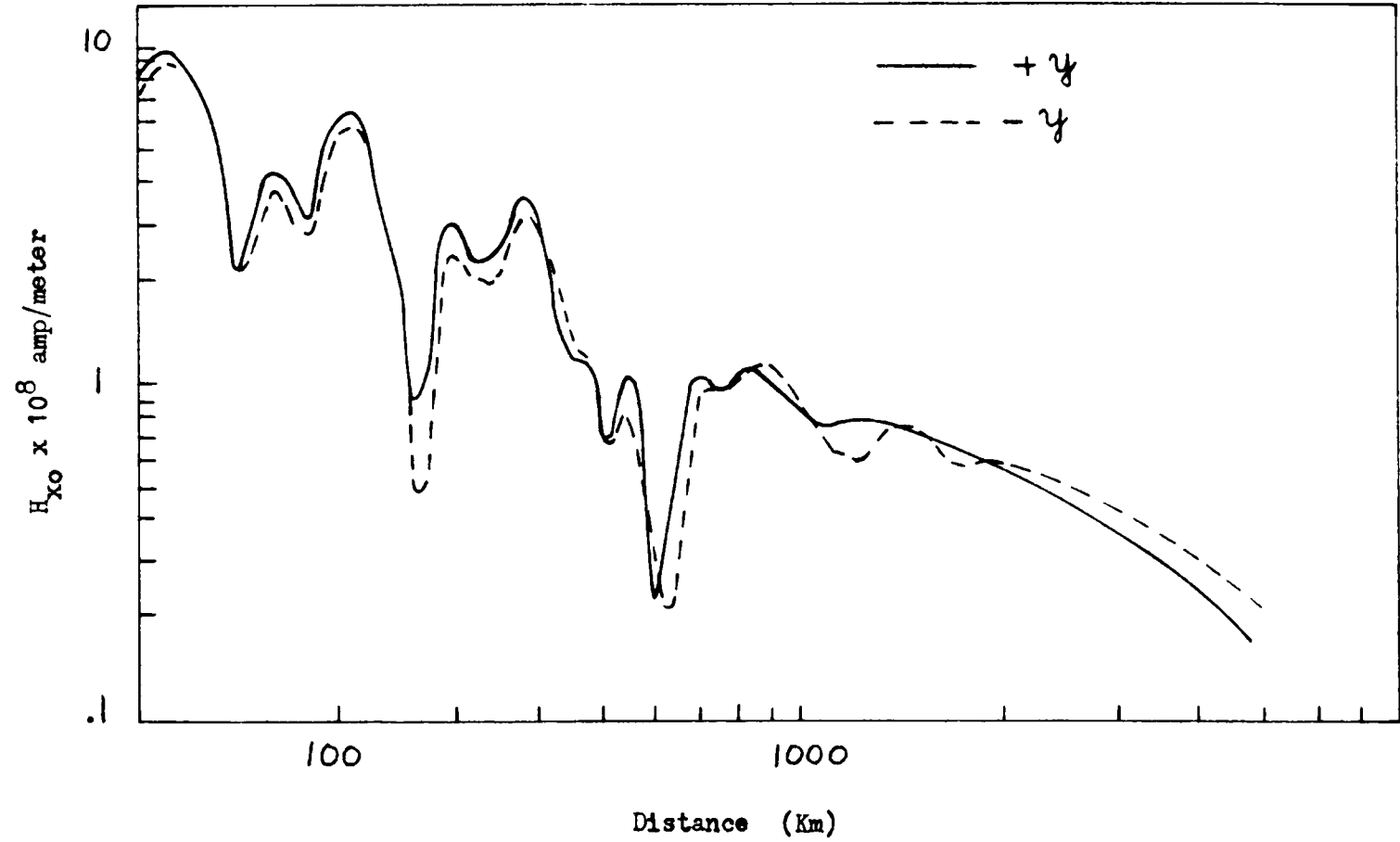


Figure 5.3 Calculated Field Strength

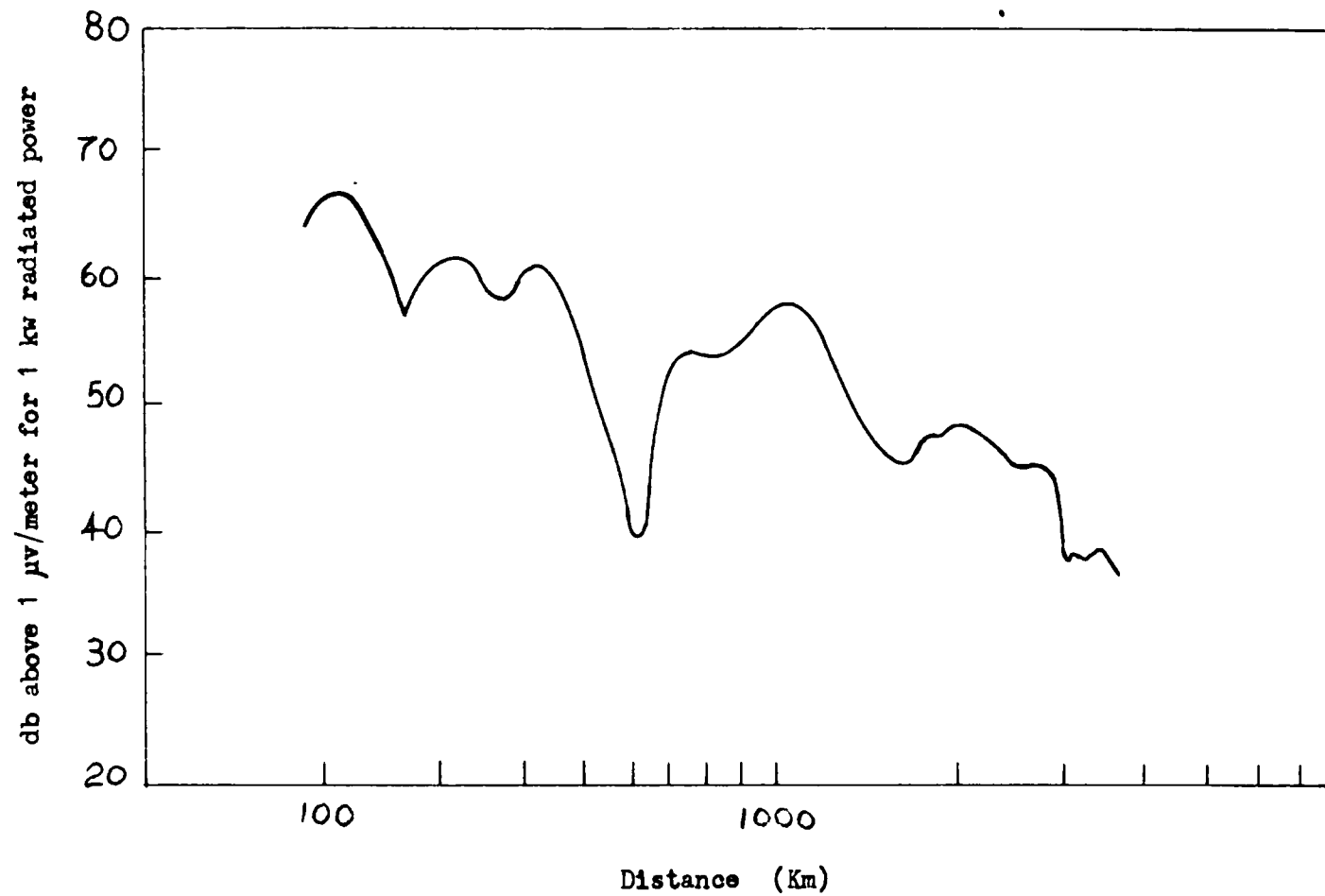


Figure 5.4 Experimental Results for 16.6 KHz

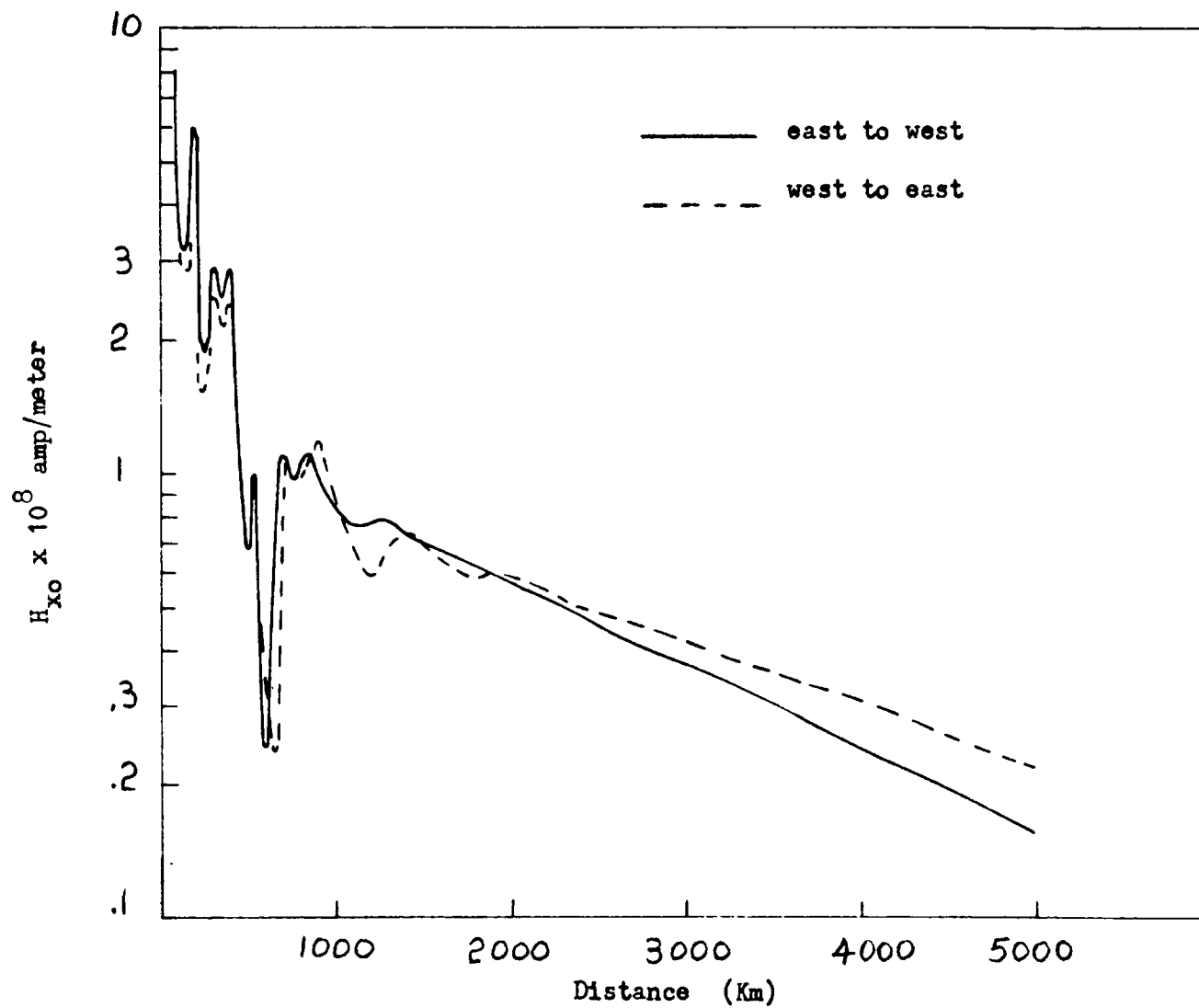


Figure 5.5 The East-West Effect



## 6. THE EAST-WEST EFFECT

### 6.1 Introduction

The theoretical field strength plots displayed in Figs. 5.1-5.5 show a pronounced difference in propagation between the  $+y$  direction and the  $-y$  direction. In particular, the attenuation for large distances is greater in the positive  $y$ -direction. This was first noted experimentally by Round et al. (1925) on a round the world cruise and has been named the east-west effect. It appears most strongly in propagation along the magnetic equator and disappears for directions due north or south.

More recently the east-west effect received a theoretical foundation through the work of Barber and Crombie (1959). It was shown that the nonreciprocity is due to the interaction between the earth's magnetic field and a component of the electric vector rotating in the vertical plane of propagation. This implies that even in the absence of an ambient magnetic field an inhomogeneous wave propagates in the ionosphere. In this chapter it will be shown not only that the wave in the ionosphere is indeed inhomogeneous, but that this is an absolute necessity for a nonreciprocity to occur. As a corollary it will be seen that for a lossless ionosphere the east-west effect will not appear.

Throughout the discussion it will be evident that the longitudinal component of the electric field in the ionosphere is responsible for the nonreciprocity appearing in the reflection coefficient.

## 6.2 Physical Concepts

Since medium (1), as well as medium (0), is reciprocal, it is clear that the boundaries must be essential in producing the nonreciprocity. At  $z = 0$  the reflection coefficient is unity which is certainly independent of direction, but at  $z = b$  the reflection coefficient is:

$$R = \frac{\chi \cos \phi_{jn} - \sqrt{\chi - \sin^2 \phi_{jn}} - iK \sin \phi_{jn}}{\chi \cos \phi_{jn} + \sqrt{\chi - \sin^2 \phi_{jn}} + iK \sin \phi_{jn}} \quad (6.1)$$

It depends on the direction of propagation because  $\sin(\phi_{jn}) = -\sin(-\phi_{jn})$ . The air ionosphere boundary, then, is necessary to produce the east-west effect. This should have been expected since expression (3.22), stating the continuity of the tangential electric field, contains an extra term dependent on direction.

An analogous problem was considered some time ago (Fry, 1928) and the results are applicable here. Fry discussed the properties of optical frequencies incident upon metals concluding that the wave penetrating into the medium is inhomogeneous. This is to say the direction of amplitude attenuation is different from the direction of phase gradient (Stratton, 1941). Furthermore, if the wave is polarized in the plane of incidence, Fry demonstrated that the electric field vector rotates in the medium. Now, the index of refraction and skin depth of metals at optical frequencies are about the same as the index of refraction and "skin depth" of the ionosphere at vlf. It could therefore be presumed that in the absence of a steady magnetic field

waves incident on the ionosphere exhibit a behavior similar to optical frequencies incident upon metals. And as will be shown, they do.

The elliptically rotating electric field vector will cause the available free electrons to describe elliptic paths in the plane of incidence. If the magnetic field is now superimposed it will alter the motion of the electrons. Depending on its direction it will either increase the electron orbit or decrease it. The electron motion in turn modifies the electric field. Thus the electric field is coupled to the steady magnetic field, in particular to its orientation, by the moving electrons. A different orientation of the steady magnetic field results in a different propagating electric field. This physical picture will now be discussed analytically.

### 6.3 Origin of the Nonreciprocity

In source-free medium (1) for harmonic time dependence Maxwell's equations become:

$$\vec{\nabla} \times \vec{E} - i\mu_0\mu\omega\vec{H} = 0 \quad (6.2)$$

$$\vec{\nabla} \times \vec{H} + i\epsilon_0\epsilon\omega\vec{E} = 0 \quad (6.3)$$

By combining (6.3) with (6.2) and taking  $\mu=1$  the vector wave equation appears:

$$(\vec{\nabla} \times \vec{\nabla} \times - k_0^2 \vec{\epsilon})(\vec{E}) = (\vec{0}) \quad (6.4)$$

The parentheses are used to denote that this equation may actually be written as a matrix equation. Since the boundary belongs more naturally into the rectangular coordinate system, it will be written as:

$$\begin{bmatrix} -(\partial_z^2 + \partial_y^2 + k_0^2 \mu_5) & 0 & 0 \\ 0 & -(\partial_z^2 + k_0^2 \epsilon) & \partial_z \partial_y - i k_0^2 \eta \\ 0 & \partial_z \partial_y + i k_0^2 \eta & -(\partial_y^2 + k_0^2 \epsilon) \end{bmatrix} \begin{bmatrix} E_x \\ E_y \\ E_z \end{bmatrix} = \begin{bmatrix} 0 \\ 0 \\ 0 \end{bmatrix} \quad (6.5)$$

In order to glean the desired information from (6.5) the following simple example will be considered. A plane wave is incident upon the air-ionosphere boundary as shown in Fig. 6.1. There will be a reflected and transmitted wave. If the space dependence of the wave is assumed to be of the form

$$e^{-i(my+nz)}$$

in either medium, then the partial derivatives in medium (1) are:

$$\partial_y = -im_1 \quad ; \quad \partial_z = -in_1$$

This means that the second equation in (6.5) may be written:

$$\frac{E_y}{E_z} = - \frac{n_1 m_1 + i k_0^2 \eta}{n_1^2 - k_0^2 \epsilon} \quad (6.6)$$

Several things may now be said. First, if  $E_z$  is normalized to unity, (6.6) is actually the longitudinal component of the electric field in the ionosphere. It is composed of a term in time phase with  $E_z$  and a term  $\frac{\pi}{2}$  radians out of time phase. As was noted in Section 6.2, the latter term gives rise to an elliptically rotating component of the electric field vector. Furthermore the longitudinal component depends upon the direction of propagation. Since  $\eta$  is complex a

change in its sign would alter the real part of (6.6) thus changing the magnitude of  $E_y$ . This change would carry into the boundary condition and thence into the reflection coefficient causing the nonreciprocity.

Secondly, if the d.c. magnetic field vanishes the wave still retains a component of the electric vector rotating in the  $y$ - $z$  plane. This is because  $\frac{n_1}{k_0}$  in the expression:

$$\left(\frac{n_1}{k_0}\right)^2 + \left(\frac{m_1}{k_0}\right)^2 = \chi$$

is complex. Because of continuity at the interface  $n_1$  equals  $n_2$  and hence is real.  $\chi$  is complex from Chapter 1. Therefore  $n_1$  is complex and the expression:

$$\frac{E_y}{E_z} = \frac{-n_1 m_1}{n_1^2 - k_0^2 \epsilon}$$

is complex which proves the assertion. (Note:  $\epsilon$  need not be complex).

It will now be shown that unless the wave propagating in the ionosphere contains an elliptically rotating component of the electric vector without the d.c. magnetic field present, there will be no east-west effect. To this end it will be assumed that the wave in the ionosphere is homogeneous, which implies among other things, that the collision frequency,  $\nu$ , be zero. Hence  $n_1$  is real instead of complex and (6.6) may be rewritten

$$\frac{E_y}{E_z} = \frac{-n_1 m_1}{n_1^2 - k_0^2 \epsilon} + \frac{i k_0^2 \eta}{n_1^2 - k_0^2 \epsilon} = A + iB$$

where both  $A$  and  $B$  are strictly real. (Since  $\nu = 0$  both  $\eta$  and  $\epsilon$  are real). If the direction of propagation changes ( $\eta \rightarrow -\eta, B \rightarrow -B$ )

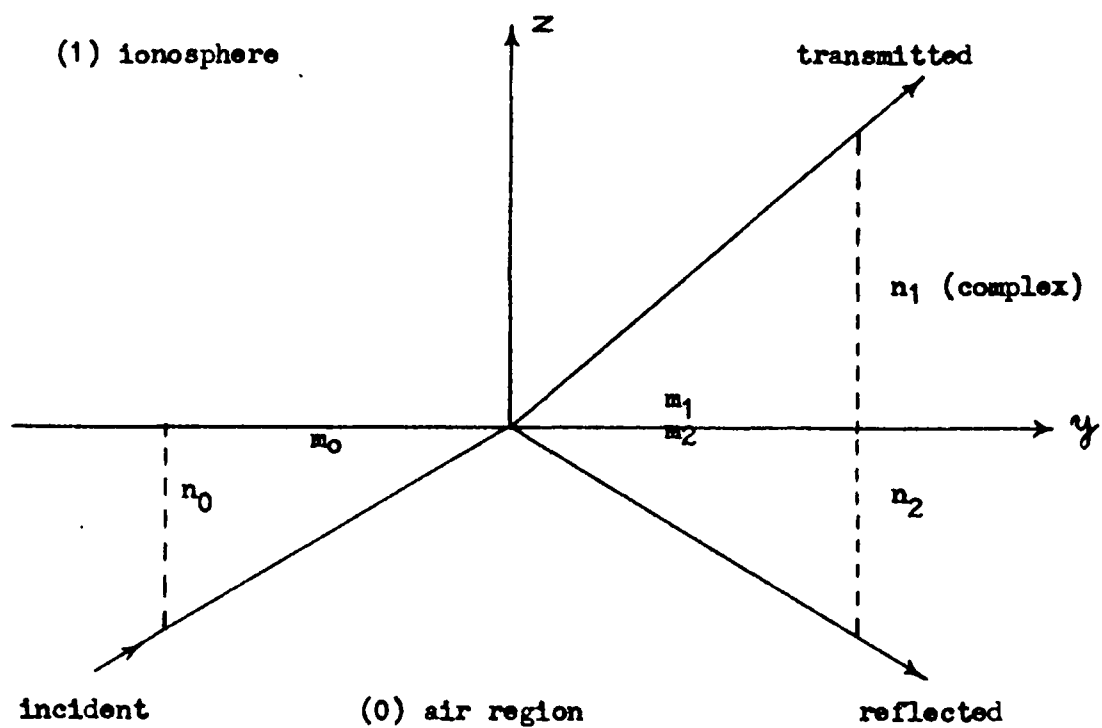


Figure 6.1 Plane Wave Incident Upon Air-Ionosphere  
Boundary

the phase relation of  $E_y$  to  $E_z$  changes, i.e. the direction of rotation in the vertical plane of propagation is reversed, But the absolute value  $|A+iB|$  remains the same. Hence the longitudinal component of the electric field in the ionosphere does not change in magnitude. This component is, of course, continuous across the boundary. Hence, in this case there is no difference between propagation east and west.

The properties just discussed for the tangential electric field under a change in direction, change in phase but constant magnitude, also appear in the reflection coefficient. If the wave is homogeneous the reflection coefficient, (6.1), may be written:

$$R = \frac{C - iD}{E + iD} = \frac{|C - iD|}{|E + iD|} e^{-i\phi_1 + i\phi_2}$$

where:

$$C = \chi \cos \phi_{jn} - \sqrt{\chi - \sin^2 \phi_{jn}}$$

$$E = \chi \cos \phi_{jn} + \sqrt{\chi - \sin^2 \phi_{jn}}$$

$$D = K \sin \phi_{jn}$$

and

$$\phi_1 = \arctan \frac{D}{C} \quad ; \quad \phi_2 = \arctan \frac{D}{E}$$

Changing the sign of  $D$  (a change either in orientation of the magnetic field or in direction of propagation) leaves  $R$  with the same absolute value but with a different phase. Hence it may be stated again that if the wave in the ionosphere were not inhomogeneous, the magnitude of the reflection coefficient would be the same for either east or west propagation, only the phase would differ.

#### 6.4 The Lossless Ionosphere

For the hypothetical case of a lossless ionosphere,  $\nu = 0$ , the east-west effect will not occur. This may be quickly seen by considering the reflection coefficient:

$$R = \frac{\chi \cos \phi_{jn} - (\sqrt{\chi - \sin^2 \phi_{jn}} + iK \sin \phi_{jn})}{\chi \cos \phi_{jn} + (\sqrt{\chi - \sin^2 \phi_{jn}} + iK \sin \phi_{jn})}$$

For  $\nu = 0$ ,  $K$  is real and

$$\chi \xrightarrow[\nu \rightarrow 0]{} S = 1 - \left(\frac{\omega_p}{\omega}\right)^2$$

Therefore  $\sqrt{\chi - \sin^2 \phi_{jn}}$  is either pure imaginary or real. For  $\frac{\omega_p}{\omega} \geq \cos \phi_{jn}$  it is imaginary and  $|R|=1$  regardless of the direction of propagation. For  $\frac{\omega_p}{\omega} < \cos \phi_{jn}$  it is real,  $|R| < 1$ , but a change in direction yields only a change in phase not in magnitude. This latter case is the same as discussed just previously.

Hence in either case the east-west effect does not occur.

#### 6.5 Conclusion

It has been seen that the wave in the ionosphere has a component of the electric vector rotating in the vertical plane of propagation. This component is an absolute necessity for the appearance of the east-west effect. If the ionosphere is considered lossless the wave does not contain this elliptically rotating component and the east-west effect does not appear.



From a mathematical viewpoint the nonreciprocity enters into the reflection coefficient because the longitudinal component of the electric field, which is continuous across the boundary, depends in magnitude upon the direction of propagation.

## 7. SUMMARY AND CONCLUSION

In the preceeding chapters the problem of vlf wave propagation along the magnetic equator has been developed. From the discussion of the boundaries in Chapter 2, it was concluded that a suitable model would be a parallel plate waveguide bounded by a perfect conductor at the bottom and an anisotropic magnetoplasma at the top.

Using this model the problem was developed in Chapter 3 and the field equations obtained. It was found that the fields were, in general, coupled by the differential equations in the magnetoplasma. In order to uncouple these the TM mode propagating along the magnetic equator was considered exclusively. In addition it was noted that the boundary conditions contain an explicit dependence upon the off-diagonal terms of the permittivity tensor.

In Chapter 4 the fields were expressed as integrals interpreted in the complex plane. It was possible to express the answer as an infinite series of integrals which were evaluated by the method of steepest descents. The resulting answers were, of course, approximate but extremely accurate at distances for which  $k_0 r \gg 1$ .

The resulting field strength plots compared favorably with actual observations. At distances close to the source large interference effects are present. These damp out farther away as the high order modes contribute less and less. It is interesting to note that even for distances as great as 2000 km the second and higher order modes

contribute to the field. The attenuation observed experimentally and that calculated agree reasonably well. The theoretical approach yielded 3.67 db/K and 2.78 db/K of attenuation for east-west and west-east propagation respectively, while experimental data yielded approximately 3-4 db/K but for random directions.

The graphs also give strong evidence of the east-west effect. This nonreciprocal behavior of the reflection coefficient at the ionosphere is discussed at length in Chapter 5. Its origin lies in the coupling at the boundary between the longitudinal component of the electric field and the steady magnetic field. The coupling is accomplished through the off-diagonal terms in the permittivity tensor, i.e. through the anisotropy of the ionosphere.

## REFERENCES

- Banos, A. (1966), Dipole Radiation in the Presence of a Conducting Halfspace, Pergamon Press, Oxford.
- Barber, N. F., and D. D. Crombie (1959), V.L.F. reflections from the ionosphere in the presence of a transverse magnetic field, J. Atmos. Terr. Phys., vol. 16, 37-45.
- Budden, K. G. (1951), The reflection of v.l.f. radio waves at the surface of a sharply bounded ionosphere with superimposed magnetic field, Phil. Mag., vol. 42, 833.
- Budden, K. G. (1954), A Reciprocity Theorem on the Propagation of Radiowaves via the Ionosphere, Proc. Camb. Phil. Soc., vol. 50, 604-613.
- Brekhovskikh, L. (1960), Waves in Layered Media (transl.), Academic Press, New York and London.
- Crombie, D. D. (1958), Differences between the east-west and west-east propagation of VLF signals over long distances, J. Atmos. Terr. Phys., vol. 12, 110-117.
- de Marchin, P. (1964), Radiation from an Infinite Axial Slot on a Perfectly Conducting Cylinder Clad with Magnetoplasma, M. S. Thesis, University of Arizona, Tucson, Arizona
- Debrott, D. and A. Ishimaru (1961), East-West Effect on VLF Mode Transmission Across the Earth's Magnetic Field, NBS Jnl. Research, vol. 65D, 47-52.
- Fry, T. C. (1928), Plane Waves of Light, Journal Opt. Soc. America, vol. 16, 1.
- Galejs, J. and R. V. Row (1964), Propagation of ELF Waves Below an Inhomogeneous Anisotropic Ionosphere, IEEE Trans. Ant. Prop. AP-12, No. 1.
- Round, H. J. T., Eckersley, T. L., Tremellon, K., and F. C. Lunnion (1925), Report on measurements made on signal strength at great distances during 1922 and 1923 by an expedition sent to Australia, J. Inst. Elect. Engrs., vol. 63, 93-101.

- Schell, R. R. (1967), On the Radiation from Sources in Layered Media Including Magnetoplasma, Ph. D. Dissertation, University of Arizona, Tucson, Arizona.
- Stratton, J. A. (1941), Electromagnetic Theory, McGraw Hill, New York.
- Tyras, G. and G. Held (1959), On the Propagation of Electromagnetic Waves Through Anisotropic Layers, IRE Trans. Ant. Prop. AP-7, special supplement, S296-S300.
- Tyras, G., Ishimaru, A., and H. M. Swarm (1963), Lateral Waves on Air-Magnetoplasma Interfaces, Electromagnetic Theory and Antennas, ed. by E. C. Jordan, Part I, pg 517, Pergamon Press, Oxford.
- Tyras, G. (1964), Radiation and Propagation of Electromagnetic Waves, Lecture Notes, University of Arizona, Tucson, Arizona.
- Wade H. D., and R. H. Williams (Jan. 1966), VLF Radiation in Air From an Electric Line Current Source Located in an Ionospheric Halfspace, Radio Science, vol. 1, No. 1.
- Wait, J. R. (1957), The Mode Theory of VLF Ionospheric Propagation for Finite Ground Conductivity, Proc. IRE, vol. 45, 760-767.
- Wait, J. R. (1962), Electromagnetic Waves in Stratified Media, Pergamon Press, Oxford.
- Wait, J. R., and H. H. Howe (1957), The Waveguide Mode Theory of VLF Ionospheric Propagation, Proc. IRE, vol. 45, 95.
- Wait, J. R., and K. Spies (1960), Influence of Earth Curvature and the Terrestrial Magnetic Field on VLF Propagation, J. Geophys. Res., vol. 65, 2325-2331.
- Yabroff, I. W. (1957), Reflection at a Sharply-Bounded Ionosphere, Proc. IRE, vol. 45, 750-753.